EurJIC European Journal of Inorganic Chemistry
ChemPubSoc Europe
MICROREVIEW

DOI: 10.1002/ejic.201((will be filled in by the editorial staff))

Mechanistic Approaches to Molecular Catalysts for Water Oxidation

Takashi Kikuchi[a] and Koji Tanaka*[a]

Keywords: Water splitting / Oxidation / Homogeneous catalysis / Electrochemistry / Reaction mechanisms / Radicals / Ruthenium

Water oxidation, where two water molecules undergo a coupled loss of four electrons and protons to form an O–O bond, is one of the most appealing target reaction for molecular catalysts in view of hydrogen production by electrolytic or photolytic water splitting in order to cope with urgent energy and environmental problems. Inspired by a natural oxygen-evolving multinuclear manganese cluster, a number of water oxidation catalysts based on multinuclear transition metal complexes have been developed during this three decades. In recent years, in parallel with discovery of mononuclear oxygen-evolving complexes, both experimental and theoretical studies have yielded important insights into the O–O bond formation pathways in these water oxidizing complexes. In this microreview, we will present an updated view of the selected current literature focusing on the working mechanism of the ruthenium-based water oxidation catalysts and on the development of rationally designed ruthenium complexes that activate water at mild potentials.

1. Introduction

Today, to address the current energy and environmental problems including the fossil fuel depletion and the global warming,[1] developments of technologies for production, storage, and utilization of energy without the consumption of fossil fuels are attracting growing attentions.[2–5] Although natural energy, such as solar and wind energy, is coming into use as a clean, sustainable, and renewable energy source, its instability of energy output and the difficulty in large-scale electricity storage have prevented its utilization as the primary energy supply. In order to overcome these drawbacks, conversion of the natural energy into the chemical bonding energy is a promising approach that enables facile energy storage and transportation, as green plants store the solar energy in carbohydrates via the photosynthetic process. Hydrogen gas is one of the most attractive energy storage owing to its high energy density and clean combustion, and hence water splitting into H_2 and O_2 by electrochemical or photochemical processes is drawing great interest. The water splitting reaction consists of two half reactions (eqs 1, 2).

[a] Institute for Integrated Cell-Material Sciences, Kyoto University, Funai Center, Kyoto University Katsura, Nishikyo-ku, Kyoto, 615-8530, Japan
Fax: +81-75-383-2812
E-mail: koji.tanaka@icems.kyoto-u.ac.jp

Takashi Kikuchi received his bachelor and master degrees in Applied Chemistry in 2006 and 2008, respectively, from the University of Tokyo, where he also obtained his Ph. D. in 2011. From 2011 to 2012, he was a postdoctoral fellow of Japan Society for Promotion of Science (JSPS) for research abroad at the Department of Chemistry of Northwestern University. He is now a researcher at the Institute for Integrated Cell-Material Sciences of Kyoto University. His research is mainly focusing on the construction and functionalization of self-assembled nanoarchitectures based on the metal coordination and the development of molecular catalysts promoting the electrochemical and photochemical reactions of gas molecules.

Koji Tanaka, after obtaining his Ph. D. in Inorganic Chemistry at Osaka University in 1975, held an Assistant Professor position at Osaka University (1971–1990) and an Associate Professor position at Osaka University (1990). From 1990 to 2012, he was a Professor at Institute for Molecular Science. He was also a Visiting Professor at the University of Strasbourg (1999) and an Adjunct Professor at Kyoto University (1999–2001, 2004–2006) and the Institute of Physical and Chemical Research (RIKEN) (1999–2001). He is now a Research Professor at the Institute for Integrated Cell-Material Sciences of Kyoto University. His research interests include coordination chemistry, electrochemistry, and molecular catalysts with particular emphasis on ruthenium complexes and transformation of gas molecules.

$2H^+ + 2e^- \rightarrow \square H_2$ ($E°$ = 0.00 V vs. SHE at pH = 0) (1)

$2H_2O \rightarrow 4H^+ \square\square\square\square$ ($E°$ = 1.23 V vs. SHE at pH = 0) (2)

The major difficulty limiting the achievable efficiency of the electrochemical water splitting is the anodic water oxidation reaction (eq 2) yielding dioxygen, since it requires the coupling of four electron and proton transfers from two H_2O molecules to form an O–O bond. Combination of four successive one-electron oxidation steps including unstable radical intermediates is highly thermodynamically demanding, and therefore, developement of rationally designed molecular catalysts capable of processing the four-electron reaction is essential to achieve the water oxidation near the thermodynamic limit ($E°$ = 1.23 V).[6–8]

In nature, an elaborate molecular catalyst, the oxygen-evolving complex (OEC) embedded in Photosystem II (PSII) performs this difficult reaction in a successive four-step process, Kok cycle.[9–11] The OEC is a tiny metal oxide cluster composed of four manganese ions, one calcium ion, and five oxygen atoms (Mn_4CaO_5), which can take five oxidation states (S_0–S_4) by the redox of the Mn ions and stores four redox equivalents.[12] Although the catalytic mechanism of the water oxidation in the OEC is still not fully understood, the catalytic transformation in the OEC is obviously one of the most important chemistries for life on the earth, and therefore, has attracted great attention of synthetic chemists challenging for mimicking the photosynthetic reactions in artificial catalytic systems.

2. Polynuclear Molecular Catalysts for Water Oxidation

Inspired by the structure of the OEC containing four Mn centers capable of storing the multiple redox equivalents, a number of molecular catalysts to conduct water oxidation based on multinuclear transition metal complexes including ruthenium (Ru)[13–26] and manganese (Mn)[27–35] have been synthesized during this three dacades (Figure 1).

The first homogeneous oxygen evolving molecular catalyst reported by Meyer and co-workers in 1982 is an oxo-bridged polypyridyl dinuclear ruthenium complex *cis*,*cis*-$[(bpy)_2(H_2O)RuORu(OH_2)(bpy)_2]^{4+}$ (bpy: 2,2′□bipyridine) (**1**), so-called "blue dimer".[13–15] The "blue dimer" evolves oxygen gas in the presence of an excess sacrificial oxidant such as $(NH_4)_2[Ce^{IV}(NO_3)_6]$ (CAN) or Co(III) with a maximum yield and turnover number (TON) of 87% and 13.2, respectively.[36] Following the paradigmatic discovery of the "blue dimer", Naruta and co-workers prepared the first example of homogeneous Mn-based water oxidation catalysts in 1994.[27,28] Electrolysis of a pincer-shaped Mn porphyrin dimer **2** in CH_3CN containing 5% H_2O at the potential range of +1.2 – +2.0 V (vs. Ag/Ag^+) results in the evolution of O_2 gas with a current efficiency of 5–17% depending on the applied potential and TON of 9.2 at a maximum. In 1999, Brudvig and co-workers also reported a dinuclear Mn complex with two oxygen bridges $[(trpy)(H_2O)Mn(\mu\text{-}O)_2Mn(OH_2)(trpy)]^{3+}$ (trpy: 2,2′:6′,2″-terpyridine) (**3**) mimicking the structure of the OEC, and demonstrated that oxidation of **3** in aqueous solution with excess NaClO gives oxygen evolution with a yield of 10% with respect to the used NaClO and TON of four.[29–32]

Yagi,[16,17] Llobet,[18–20] and Thummel[21,22] groups have synthesized dinuclear Ru complexes **4**, **5**, and **6**, respectively, and demonstrated the catalytic water oxidation in moderate yields and TONs in the presence of the complexes using excess CAN. The oxo-bridged polyammine complex **4** shows the catalytic activity not only in the homogeneous aqueous conditions, but also in a heterogeneous system where the catalyst is embedded in an ion exchange membrane. McKenzie and co-workers reported a dinuclear Mn complex **7** in 2005, which can evolve oxygen with TON of 10–20 in the presence of *tert*-butyl hydroperoxide (TBHP) as a sacrificial oxidant.[33] CAN is not a very good oxidant in the case of **7** because the highly acidic media prevents the formation of high-valent Mn species.

In 2010, Sun and co-workers synthesized a dinuclear Ru complex **8** bridged by a rigid 3,6-bis(2′-pyridyl)pyridazine derivative, in which two Ru ions are fixed in a syn configuration with respect to the rod-like ligand.[23] The complex **8** exhibits a remarkable catalytic activity in the water oxidation in an aqueous solution of CAN with TON of 10,400, which is more than double for that of an anti counterpart (4,700).[24] In addition, in 2008, Hill and Bonchio groups have independently, nearly simultaneously revealed that a purely inorganic framework incorporating tetraruthenium core, namely a polyoxometalate $[\{Ru_4(\mu\text{-}O)_4(\mu\text{-}OH)_2(H_2O)_4\}(\gamma\text{-}SiW_{10}O_{36})_2]^{10-}$ (**9**), works as an oxygen-evolving catalyst.[25,26] Treatment of **9** with excess CAN in an acidic aqueous solution results in efficient O_2 generation with a yield of 90% and TON of 500.

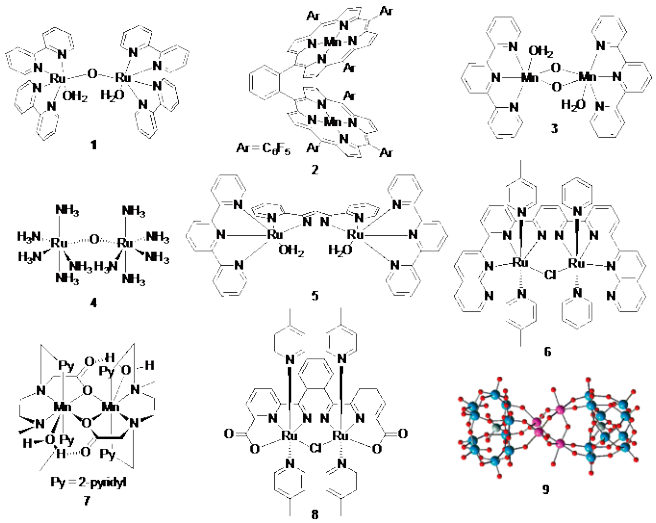

Figure 1. Molecular structures of water oxidation catalysts based on multinuclear Ru and Mn complexes.

3. Mononuclear Catalysts for Water Oxidation

Although it had been believed for a long time that the multinuclear structure is essential for the catalytic O–O bond formation, in 2008, three groups have reported that mononuclear ruthenium and iridium (Ir) complexes have catalytic activity comparable to that of the dinuclear ones in the water oxidation (Figure 2). Bernhard and co-workers have reported that a

mononuclear aquo iridium (Ir) complex $[Ir(ppy)_2(OH_2)]^+$ (Hppy: 2-phenylpyridine) **10** exhibits catalytic activity in the water oxidation.[37] The complex **10** furnishes O_2 upon addition of CAN with a volume of one-third of the expected one for complete conversion and TON of more than 2,000. Thummel and co-workers have shown that $[Ru(trpy)(bpy)Cl]^+$ **11** catalyzes the water oxidation in the presence of CAN at pH 1 to give TON of 1,170.[38] Meyer and co-workers have demonstrated that mononuclear aquo Ru complexes $[Ru(trpy)(bpm)(OH_2)]^{2+}$ (bpm: 2,2′-bipyrimidine) (**12**) and $[Ru(trpy)(bpz)(OH_2)]^{2+}$ (bpz: 2,2′-bipyrazine) generate quantitative amount of oxygen with respect to used CAN although the TONs are not very high.[39,40] In 2009, Sakai group also reported the catalytic water oxidation by an aquo Ru complex $[Ru(trpy)(bpy)(OH_2)]^{2+}$ (**13**) with excess CAN with TON of 178 in 90% yield.[41,42]

Following these discoveries of the mononuclear water oxidation complexes, Crabtree and co-workers have synthesized an Ir complex $[Ir(Cp^*)(ppy)Cl]$ (HCp^*: 1,2,3,4,5-pentamethylcyclopentadiene) (**14**) and revealed that **14** works as a water oxidation catalyst.[43] Addition of excess CAN into an aqueous solution of **14** at pH 1 results in quick generation of O_2 gas (TON > 1,500 after 5.5 hours). Albrecht and co-workers have found that an Ir complex **15** bearing a carbene-type ligand as a strong donor efficiently catalyzes water oxidation in the presence of CAN (TON 10,000 after 120 h).[44] In 2012, Sun and co-workers have reported a highly active oxygen-evolving mononuclear Ru complex $[Ru(bda)(ptz)_2]$ (H_2bda: 2,2′-bipyridine-6,6′-dicarboxylic acid; ptz: phthalazine) (**16**) by refining a similar catalyst $[Ru(bda)(pic)_2]$ (pic: 4-picoline) they previously found in 2009.[45–47] The complex **16** almost quantitatively evolves O_2 by addition of CAN with TON as high as 55,400. They also applied these Ru catalysts to photocatalytic water splitting by depositing the complex onto the TiO_2-modified FTO (fluorine-doped tin oxide) electrode together with a $[Ru(bpy)_3]^{2+}$ derivative as a photosensitizer, and accomplished TON of ca. 500 with an external bias (0.2 V vs. SHE) in a nearly neutral aqueous solution.[48]

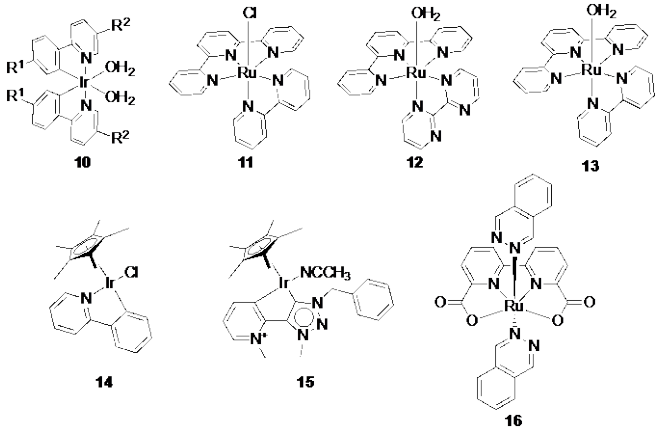

Figure 2. Molecular structures of water oxidation catalysts based on mononuclear Ru and Ir complexes.

In very recent years, in addition to the noble metal-based catalysts described above, discrete multi- and mononuclear complexes including first-row transition metals other than Mn, namely cobalt (Co),[49–52] copper (Cu),[53] and iron (Fe),[54–57] have been coming into application as the water oxidation catalysts (Figure 3). For instance, Hill and co-workers have found in 2010 that a polyoxometalate incorporating a tetranuclear cobalt core $[Co_4(H_2O)_2(PW_9O_{34})_2]^{10-}$ (**17**) oxidizes water to oxygen in nearly neutral phosphate buffer (pH 8) in the presence of $[Ru(bpy)_3]^{3+}$ as an oxidant with a yield and TON of 67% and 78, respectively.[49] Mayer and co-workers have discovered catalytic activity of a quite simple Cu complex $[Cu(bpy)(OH)_2]$ (**18**), which is prepared in situ from $Cu(OAc)_2$ and bpy in a basic aqueous solution (pH 12.5). Controlled-potential electrolysis at +1.35 V (vs. SHE) of **18** with an ITO working electrode furnishes O_2 with a quantitative Faradaic efficiency (TON > 30).[53] Costas and co-workers have demonstrated that an iron complex chelated by a tetradentate nitrogen ligand (**19**) efficiently evolves oxygen in the presence of $NaIO_4$ or CAN, in which the TONs are 1,050 and 360, respectively, for the two oxidants.[54] The properties of the water oxidation molecular catalysts described above are summarized in Table 1.

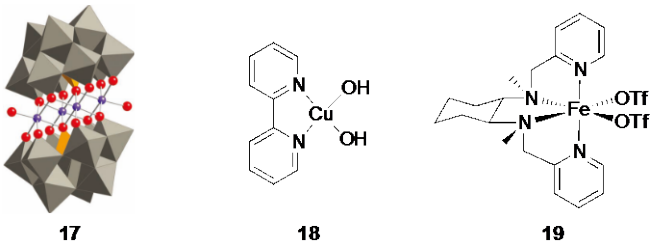

Figure 3. Molecular structures of water oxidation catalysts based on the first-row transition metal complexes.

Table 1. Water oxidation catalysts based on discrete metal complexes.

Catalyst	Oxidant	Yield[a] / %	TON[b,c]	Ref.
1	CAN	87	13.2	[36]
2	electrolysis	5–17	9.2	[27]
3	NaClO	10	4	[29]
4	CAN	–[d]	–[d]	[16]
5	CAN	73	18.6	[18]
6	CAN	–[d]	538	[23]
7	TBHP	–[d]	10–20	[33]
8	CAN	–[d]	1,700	[24]
9	CAN	90	500	[26]
10	CAN	37	2,760	[37]
11	CAN	–[d]	1,170	[38]
12	CAN	100	7.5	[39]
13	CAN	90	178	[41]
14	CAN	–[d]	1,500	[43]
15	CAN	–[d]	10,000	[44]
16	CAN	>90	55,400	[45]
17	$[Ru(bpy)_3]^{3+}$	67	78	[49]
18	electrolysis	90	>30	[53]
19	$NaIO_4$	–[d]	1,050	[54]
trans-**20**	CAN	–[d]	3,500	[81]
trans-**20**	electrolysis	–[d]	30	[81]
cis-**20**	CAN	–[d]	1,200	[81]
cis-**20**	electrolysis	–[d]	6	[81]
22	electrolysis	95	33,500	[96]
23	CAN	–[d]	414	[99]
23	electrolysis	–[d]	2.6	[99]

[a]Current efficiency in the case of electrolysis. [b]Turnover number: molar ratio of the evolved oxygen with respect to the used catalyst. [c]Although turnover frequency (TON per unit time) is also used as a characteristics of the catalyst, it often depends on the oxidant concentration. [d]Not reported.

4. Proposed Mechanism for the O–O Bond Formation

Although a number of homogeneous molecular catalysts for water oxidation based on the multinuclear and mononuclear metal complexes have been developed, their mechanisms of the O–O bond formation are still largely remained obscure. Since its discovery in 1992, the reaction mechanism of the "blue dimer" **1** and related ruthenium complexes has been enthusiastically studied by several groups both experimentally and computationally, and three prominent types of the transformation mechanisms have been advocated so far (Scheme 1).[6,42,58–80]

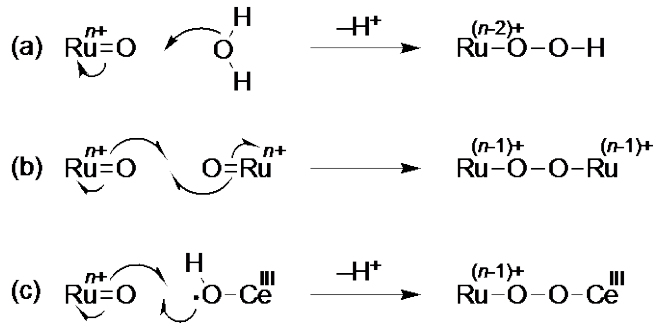

Scheme 1. Possible pathways of the O–O bond formation in the catalytic water oxidation by ruthenium-oxo complexes. (a) A electrophilic attack of the oxo ligand to the water molecule, (b) coupling of the two ruthenium-oxo species, and (c) coupling between the ruthenium-oxo and hydroxocerium species.

The O–O bond formation in the catalytic cycle of the water oxidation by the "blue dimer" has been the subject of controversy. The addition of Ce(IV) to the "blue dimer" $[(bpy)_2(H_2O)Ru^{III}ORu^{III}(OH_2)(bpy)_2]^{4+}$ (hereafter denoted $[H_2O–Ru^{III}Ru^{III}–OH_2]^{4+}$) causes successive oxidation of the Ru centers coupled with deprotonations of the aqua ligands to give two key intermediates, $[O=Ru^{IV}Ru^{V}=O]^{3+}$ and $[O=Ru^{V}Ru^{V}=O]^{4+}$. The electrophilic attack of the oxygen atom of the Ru(V)=O group in the intermediates to water molecule leads to formation a Ru^{III}–OOH bond (Scheme 1a). Meyer and Hurst groups have proposed that this "acid-base" mechanism between the high Ru^{V}=O and H_2O is the predominant pathway of the O–O bond formation not only in the dinuclear "blue dimer"[59,60,64] but also in the mononuclear Ru catalysts.[66] Hurst and co-workers have also proposed another pathway including non-innocent involvement of the bpy lidand of the "blue dimer", where Ru-assisted hydration of the bpy generates a bpy peroxide species leading to the O_2 release.[67] Sun[68], Fukuzumi[69], and Bonchio[70] and their co-workers have also revealed that the "acid-base" mechanism including Ru^{V}=O species as a key intermediate is the facile O–O bond formation mechanism in their mononuclear aquo Ru complex and mononuclear and tetranuclear Ru-cored polyoxometalates, respectively, by utilizing both experimental and theoretical approaches. In contrast, Hill and co-workers computationally proposed that the "acid-base" water activation by the Ru^{V}=O species, which is in resonance with Ru^{IV}–O•, is highly endothermic and does not occur in their multinuclear Ru-centered polyoxometalate.[71]

On the other hand, Llobet and co-workers have proposed an alternative pathway of the O–O bond formation in a dinuclear Ru catalyst $[(trpy)(H_2O)Ru^{II}(\mu\text{-bpp})Ru^{II}(OH_2)(trpy)]^{3+}$ (Hbpp: 3,5-bis(2-pyridyl)pyrazole) (**5**).[19,77,78] In analogy to "blue dimer", the oxidation of the Ru centers of $[H_2O–Ru^{II}Ru^{II}–OH_2]^{3+}$ by CAN conjugated with deprotonations of the aqua ligand gives an oxo Ru^{IV} species $[O=Ru^{IV}Ru^{IV}=O]^{3+}$. The kinetic study and isotope labelling experiments have evidenced that the O–O bond formation proceeds in a bimolecular coupling mechanism between two Ru=O species (Scheme 1b).

Furthermore, it is fairly curious that most of water oxidation reactions catalyzed by Ru complexes have been conducted by using Ce(IV), but do not proceed under the electrolysis at potentials more positive than 1.50 V. Taking into account the fact that the (Ce^{III}/Ce^{IV}) redox couple is +1.37 V (vs. SCE) in H_2O (1 M), Sakai and co-workers proposed that Ce(III)–OH•, which is in resonance with Ce(IV)–OH^- in water, works as the oxygen donor in the O–O bond formation (Scheme 1c).[42] Berlinguette and co-workers also pointed the unusual role of CAN, especially the involvement of the nitrate anion of CAN in the O–O bond formation step.[79,80]

5. Comparison between Chemical and Electrochemical Oxidation of Water

Smooth formation of Ru(IV)=O species through the well-established electron and proton loss reactions of the corresponding Ru(II)–OH_2 is a primary reason why aqua-Ru(II) complexes are predominantly used as catalyst precursors in water oxidation. Energy consumption in water oxidation must be largely dependent on the oxidation potential of Ru(IV)/Ru(V) couple by considering the role of Ru(V)=O in the O–O bond formation. A metalacyclic ligand linked to Ru with strong σ□donor carbon would cause negative shifts of the oxidation potential to create Ru complexes in a higher oxidation state. Along this line, 2-(pyrid-2′-yl)-acridine (pad) is introduced into Ru complexes to facilitate the negative shift of their oxidation potentials.[81–84]

The cyclic voltammogram (CV) of $[Ru(pad)(bpy)_2]^+$ in dry CH_3CN exhibits two reversible (Ru^{II}/ Ru^{III}) and (Ru^{III}/ Ru^{IV}) redox couples at $E_{1/2}$ = +0.52 V and +0.78 V (vs. SCE), respectively. A broad cathodic wave of the (pad/pad•−) couple appears at –1.61 V as a shoulder of the two (bpy/bpy•−) couples at $E_{1/2}$ = –1.64 V and –1.92 V. The –1.61 V cathodic wave undergoes a positive shift with increasing amounts of water, and emerges at –1.10 V in CH_3CN/H_2O (9:1 v/v). The exhaustive electrolysis of the resultant solution at –1.20 V consumes 2 F·mol^{-1} of electrons, and a hydrogenated form $[Ru(padHH)(bpy)_2]^+$ (padHH: 2-(pyrid-2′-yl)-9,10-dihydroacridine) is obtained in an almost quantitative yield. The ^{13}C NMR signals of the coordinated carbons of $[Ru(pad)(bpy)_2]PF_6$ and $[Ru(padHH)(bpy)_2]PF_6$ appear at 127.27 ppm and 126.57 ppm, respectively, that are consistent with Ru–C type single bond character.

On the other hand, protonation of pad of $[Ru(pad)(bpy)_2]^+$ by an addition of HCl causes the ^{13}C NMR signal to shift downfield to 228.87 ppm. The X-ray analysis of the protonated form, $[Ru(padH)(bpy)_2]Cl_2·10H_2O$, revealed the short Ru–C bond (2.011(4) Å) that is a significant feature of carbene type behavior. These results indicate that protonation of the non-bonded nitrogen of the cyclometalated Ru-pad effectively lowers the energy level of the π^*-orbital of pad, which gives rise to nearly two-electron transfer from Ru(II) to padH. In other words, a quinoid structure is induced, and the Ru^{II}–C and Ru^{IV}=C bonding modes exist as

contributing structures in the canonical form of $[Ru(padH)(bpy)_2]^{2+}$ (Scheme 2). The ΔH^0 and ΔS^0 values between the contributing structures including Ru^{II}–C bond and Ru^{IV}=C coordination modes were determined as –4.93 kcal·mol^{-1} and –21.82 cal·K^{-1}·mol^{-1} respectively, based on the temperature dependent ^{1}H NMR of $[Ru(pad)(bpy)_2]PF_6$ in the presence of one equivalent of HCl.

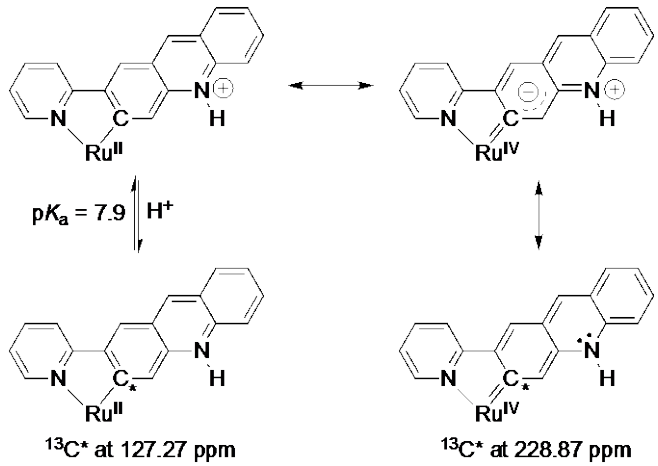

Scheme 2. Protonation-induced generation of the Ru^{IV} species in the Ru-pad complex by the resonance between the Ru^{II}–C and Ru^{IV}=C structures.

The reaction of $[Ru(pad)(CH_3CN)_4]^{2+}$ with trpy selectively gives *trans*-$[Ru(trpy)(pad)(CH_3CN)]^+$ with the orientation of the coordinating carbon trans to CH_3CN. Hydrolysis of *trans*-$[Ru(trpy)(pad)(CH_3CN)]^+$ produces *trans*-$[Ru(trpy)(pad)(OH_2)]^+$ (*trans*-[**20**]$^+$) stereospecifically. Irradiation of visible-light (λ > 420 nm) to *trans*-[**20**]$^+$ in acetone-d_6 results in complete isomerization to *cis*-$[Ru(trpy)(pad)(OH_2)]^+$ (*cis*-[**20**]$^+$) in two hours at room temperature.

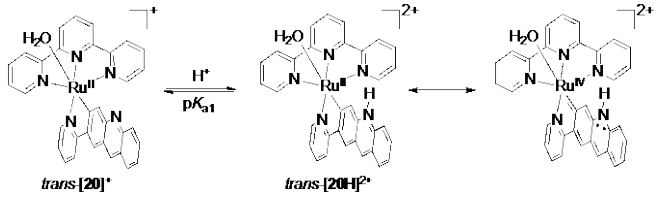

Scheme 3. Resonance structures of *trans*-[**20H**]$^{2+}$ including the contribution of Ru^{IV} species.

Trans- and *cis*-[**20**]$^+$ exhibit two types of acid-base equilibrium reactions. One is the protonation of the non-bonded nitrogen of pad (pK_{a1}) (Scheme 3), and the other is the proton dissociation of Ru–OH_2 (pK_{a2}). The pK_{a1} and pK_{a2} of *trans*-[**20**]$^+$ determined by pH titration are 6.90 and 10.03, respectively. Those values of the cis isomer are 6.75 and 11.01. The CV of *trans*-[**20**]$^+$ in an aqueous solution at pH 1.95 exhibits a broad redox couple at 0.31 V and *cis*-[**20**]$^+$ at 0.33 V (vs. SCE). Strong anodic currents begin to flow at the potentials more positive than +1.4 V as a consequence of water oxidation. The initial oxidation process in the isomer *trans*-[**20H**]$^{2+}$ (within the pH range of 1.95–4.0) is a pH independent 2e$^-$ process of $[Ru(trpy)(=padH)(OH_2)]^{2+}$/$[Ru(trpy)(=padH)(OH_2)]^{4+}$ couple. The same oxidation process shifts by –30 mV/pH in a pH range from 4 to 7, and by –60 mV/pH from pH 7 to pH 11, which indicates that these waves are corresponding to a 2e$^-$/1H$^+$ and 2e$^-$/2H$^+$ processes, namely $[Ru(trpy)(=padH)(OH_2)]^{2+}$/$[Ru^{IV}(trpy)(pad)(OH_2)]^{3+}$ and $[Ru^{II}(trpy)(pad)(OH2)]^+$/$[Ru^{IV}(tpy)(pad)(=O)]^+$ couples, respectively. The bulk electrolysis of *trans*-[**20**]$^+$ conducted at +0.60 V consumes 2F·mol^{-1} electrons in buffer solutions at various pH (2–10).

Treatment of the complex with CAN in aqueous in 0.1 M HNO_3 catalytically evolves O_2. The TON values for O_2 evolution by *trans*- and *cis*-[**20**]$^+$ are 3,500 and 1,200, respectively. The initial rate is proportional to the first order with respect to the concentrations of Ce(IV) and the complex. Compared to the catalytic abilities of mononuclear ruthenium aqua complexes reported so far, *trans*-[**20**]$^+$ has remarkable ability for the dioxygen evolution from water (Table 1). Furthermore, both complexes also catalyze water oxidation under the electrolysis at +1.40 V vs. SCE in water at pH 4.0 (buffered with H_3PO_4/KOH) (Figure 4). However, O_2 evolution by electrochemical water oxidation is very scarce compared to the chemical oxidation using Ce(IV) although the redox potential of the Ce(IV)/Ce(III) pair of CAN is reported to be in a range of +1.20 – +1.46 V (vs. SCE) depending on conditions. The catalytic activity of the *trans*-[**20**]$^+$ (TON 30) is also higher than *cis*-[**20**]$^+$ (TON 6). The higher catalytic ability of *trans*-isomer is correlated with the lower pK_{a2} value compared to *cis*-isomer as a consequence of the contribution by trans effect of the σ-donating and π-accepting ability of carbon coordination. It leads to destabilization of the Ru–OH_2 bond and induction of a partial positive character at the oxygen atom of the aqua ligand, which allows the attack by another water molecule to evolve dioxygen. This is a rare example of electrolytic O_2 evolution molecular catalysts working under +1.40 V vs. SCE.[53,85]

It is concluded that O_2 evolution in the electrochemical oxidation of *trans*- and *cis*-[**20**]$^+$ proceed via the nucleophilic attack of water molecule to Ru=O species. However, the substantial differences in the catalytic activity of *trans*- and *cis*-[**20**]$^+$ toward O_2 evolution between the chemical oxidation using Ce(IV) (TON 3,500 and 1,200) and electrochemical oxidation (TON 30 and 6) cast suspicion on the possibility of the occurrence of the reaction of Ru(V)=O with Ce^{III}-OH$^\bullet$ affording Ru-O-OH bonds besides the role of one-electron oxidant.[42]

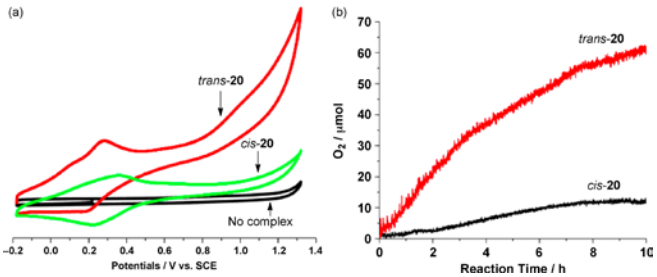

Figure 4. (a) Catalytic dioxygen evolution by the complexes at pH 4. (b) Dioxygen evolutions by *trans*- and *cis*-**20** in electrochemical method at pH 4 and potential 1.40 V (vs. SCE).

6. Water Activation on Low-Valent Ru Centers as a Stabilized Oxyl Radical

Dioxolene is an electrochemically non-innocent ligand, which takes three distinct electronic states classified as quinone (Q), semiquinone (Sq), and catecholate (Cat), and its metal complex often shows strong electronic interactions between the metal center and the ligand.[86–88] In the case of ruthenium–dioxolene complexes, charge distribution between the Ru center and the

ligand takes place to allow the resonance hybridization among Ru^{n+}–Q, $Ru^{(n+1)+}$–Sq, and $Ru^{(n+2)+}$–Cat (Scheme 4a) as a consequence of the close energy levels of the t_{2g} (dπ) orbitals of ruthenium and the pπ* orbital of the dioxolene ligand.[89–92] For example, the energy gap between the Ru(II)–Bu_2Q and Ru(III)–Bu_2Sq structures are so small that it is quite difficult to determine which of them the ground state is experimentally, or even theoretically. Nor magnetic analysis can distinguish these two species as a consequence of the antiferromagnetic interaction between two unpaired electrons on the Ru(III) and Sq units, which makes Ru(III)–Bu_2Sq a diamagnetic state.

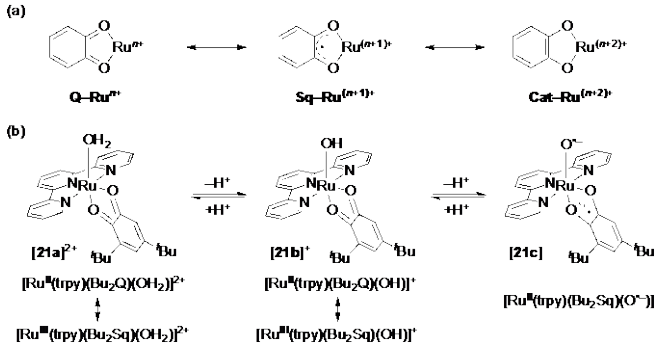

Scheme 4. (a) Electronic structures of the ruthenium-dioxolene complex including charge distribution between the metal center and the ligand. (b) Formation of the ruthenium oxyl radical complex $[Ru^{II}(trpy)(Bu_2Sq)(O^{\bullet-})]$ **21c** via intramolecular electron transfer coupled with acid-base equilibrium.

In 2003, Tanaka and co-workers reported the first preparation and characterization of a stable ruthenium oxyl radical complex $[Ru^{II}(trpy)(Bu_2Sq)(O^{\bullet-})]$ (Bu_2Sq: 3,5-di-*tert*-butyl-1,2-benzosemiquinone) ([**21c**]) by the double deprotonation of the aqua ligand of $[Ru^{II}(trpy)(Bu_2Q)(OH_2)](ClO_4)_2$ ([**21a**]$(ClO_4)_2$) (Scheme 4b).[93,94] The aquo complex $[\mathbf{21a}]^{2+}$ shows a strong absorption band at 600 nm in CH_2Cl_2, derived from a charge transfer (CT) between the Ru center and the dioxolene ligand. After single deprotonation of the aqua ligand of $[\mathbf{21a}]^{2+}$ by addition of one equivalent of *t*-BuOK, the CT band shifts to 576 nm (Figure 5), indicating formation of a hydroxo complex $[Ru^{II}(trpy)(Bu_2Q)(OH)](ClO_4)$ ([**21b**](ClO_4)). Addition of more than three equivalents of *t*-BuOK diminishes the absorption band at 576 nm, and a new band emerges at 870 nm, which is characteristic of the Ru(II)–Sq species.

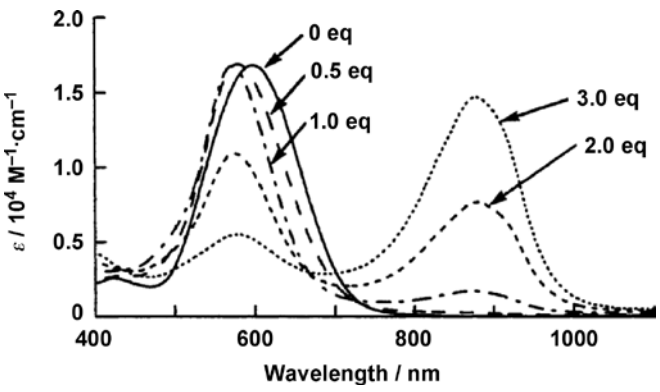

Figure 5. Electronic absorption spectra of $[Ru^{II}(trpy)(Bu_2Q)(OH_2)](ClO_4)_2$ ([**21a**]$(ClO_4)_2$) in the presence of various equivalents of *t*-BuOK in CH_2Cl_2.

Combination with the results of EPR, CV, and X-ray crystallographic analysis revealed that the deprotonation of the hydroxo ligand of $[\mathbf{21b}]^+$ affords the ruthenium oxyl radical complex [**21c**]. The EPR experiments confirm that the ground state of [**21c**] is a triplet biradical, indicating antiferromagnetic interaction between the oxyl radical and the semiquinone ligand. The acid-base equilibrium of the hydroxo ligand formally gives an oxo ligand O^{2-}, and the accompanying intramolecular electron transfer from the resultant oxo ligand to the quinone ligand facilitates the formation of the oxyl radical species, Sq–Ru(II)–$O^{\bullet-}$. Considering that proton abstraction from aquo or hydroxo complexes by strong bases usually gives μ-oxo bridged complexes (M–O–M), the strong electronic interaction between Ru and the dioxolene ligand plays a critical role in the remarkable stabilization of the oxyl radical. While the generation of the reactive species from Ru–OH_2 without any non-innocent ligands (e.g., the "blue dimer") requires the oxidation up to the high oxidation state Ru(V)=O, the dioxolene ligand as an electron pool enables the formation of the reactive oxyl radical species at the lower oxidation state Ru(II). Although the oxyl radical complex [**21c**] does not exhibit oxidative activity for organic substrates, one electron oxidation by Ag(I) affords Q–Ru(II)–$O^{\bullet-}$ (or Sq–Ru(III)–$O^{\bullet-}$) species that can oxidize various cyclic dienes to give the corresponding aromatic compounds and Q–Ru(II)–OH.[95]

One can imagine that if two Q–Ru–OH_2 moieties are fixed in spatial proximity by using a suitable bridging ligand and rendered to Sq–Ru–$O^{\bullet-}$ species by an intramolecular electron transfer conjugated with acid-base equilibrium, radical coupling between the two oxyl radicals will take place to form an O–O bond. Based on this concept, Tanaka group developed a dinuclear ruthenium complex $[Ru^{II}_2(btpyan)(Bu_2Q)_2(OH)_2]^{2+}$ $[\mathbf{22}]^{2+}$ (btpyan: 1,8-bis(2,2′:6′,2″-terpyrid-4′-yl)anthracene; Bu_2Q: 3,6-di-*tert*-butyl-1,2-benzoquinone) (Figure 6), and demonstrated its extraordinarily high catalytic activity for the electrolytic four-electron oxidation of water to dioxygen.[96–98] The two OH groups direct into the cavity as a consequence of the rigid framework of the btpyan ligand, where the two terpyridyl units are arranged in parallel in close positions (the distance between the central nitrogen atoms is 4.22 Å), and steric hindrance of the bulky *tert*-butyl groups of the quinone ligand. The dinuclear complex $[\mathbf{22}]^{2+}$ shows a strong CT absorption at 576 nm in MeOH as is observed in the mononuclear counterpart $[\mathbf{21b}]^+$. Deprotonation of the hydroxo ligands of $[\mathbf{22}]^{2+}$ by two equivalents of *t*-BuOK decreases the absorption at 576 nm, and a new band appears at 850 nm, indicating the generation of the Sq–Ru(II)–$O^{\bullet-}$ species via the intramolecular electron transfer coupled with the acid-base equilibrium of the hydroxo ligand. Although two oxyl radicals sit closely within the cavity of the btpyan framework in the resultant tetraradical complex $[Ru^{II}_2(btpyan)(Bu_2Sq)_2(O^{\bullet-})_2]$, it exists as a stable compound, and the radical coupling to form an O–O bond does not take place.

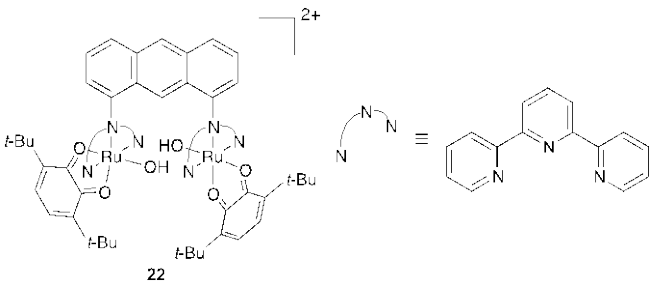

22

Figure 6. Molecular structure of $[Ru_2(btpyan)(Bu_2Sq)_2(OH)_2]^{2+}$ ($[\mathbf{22}]^{2+}$).

A controlled-potential electrolysis of $[\mathbf{22}](SbF_6)_2$ modified on an ITO electrode conducted at +1.70 V (vs Ag/AgCl) in water (pH 4.0) results in O_2 gas evolution with current efficiency of 95% and a fairly high TON of 33,500.[96] The complex $[\mathbf{22}]^{2+}$ modified on the plate is also smoothly converted to the bis(oxyl radical) species at pH higher than 3.0 owing to the proton dissociation. The CV of the deposited $[\mathbf{22}]^{2+}$ in water (pH 4.0) shows a broad redox wave at +0.32 V (vs. Ag/AgCl) and an irreversible anodic wave at +1.19 V, that are assigned to $[Ru^{II}–Sq]/[Ru^{III}–Sq]$ and $[Ru^{III}–Sq]/[Ru^{III}–Q]$ couples, respectively. Moreover, a strong anodic current is observed at potentials more positive than +1.2 V, which apparently derives from the catalytic water oxidation. During the electrolysis of $[\mathbf{22}]^{2+}$ modified on the ITO electrode at +1.70 V, the current gradually decreases as a consequence of the acidification of the solution, and almost stops at pH 1.2. The water oxidation resumes after readjustment of pH to 4.0 by addition of KOH to the aqueous solution. The water oxidation continues to evolve 33,500 O_2 molecules per one $[\mathbf{22}]^{2+}$ molecule until the complex exfoliates from the electrode surface, which indicates the high stability of $[\mathbf{22}]^{2+}$ in the solid state.

On the other hand, $[Ru^{III}_2(btpyan)(bpy)_2(\mu\text{-}Cl)]^{3+}$ ($[\mathbf{23}]^{3+}$), in which the dioxolene ligands of $[\mathbf{22}]^{2+}$ are replaced by bpy ligands, exhibits much lower catalytic activity in the water oxidation, which supports critical involvement of the oxyl radical species in the catalytic water oxidation by $[\mathbf{22}]^{2+}$.[99] The CV of $[\mathbf{23}]^{3+}$ at pH 1.0 exhibits two reversible redox waves at +0.61 V and +0.80 V (vs. Ag/AgCl) that are ascribed to $[Ru^{II}–Ru^{II}]/[Ru^{II}–Ru^{III}]$ and $[Ru^{II}–Ru^{III}]/[Ru^{III}–Ru^{III}]$ couples, respectively. A pH dependency of the latter redox couple suggests that the bridging Cl ion is substituted by water molecules in the $[Ru^{III}–Ru^{III}]$ state. A controlled-potential electrolysis of $[\mathbf{23}]^{3+}$ in a phosphate buffer solution (pH 2.6) at +1.6 V catalytically evolves dioxygen, but the TON is quite low (2.6). Resonance Raman spectra of $[\mathbf{23}]^{2+}$ after the electrolysis at +1.40 V in $H_2{}^{16}O$ show two Raman bands at 442 and 842 cm^{-1}, which shift to 426 and 780 cm^{-1} in $H_2{}^{18}O$, respectively. The isotopic frequency shifts are consistent with the calculated values of the Ru–O and O–O stretching modes, respectively, indicating formation of an intermediate including Ru–O–O–Ru moieties. Although addition of excess CAN to the acidic solution of $[\mathbf{23}]^{3+}$ (pH 1.0) allows evolution of more volume of dioxygen, the TON of 414 is still not very high.

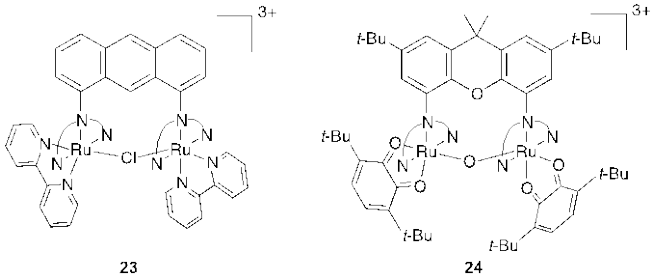

Figure 7. Molecular structures of $[Ru_2(btpyan)(bpy)_2(\mu\text{-}Cl)]^{3+}$ ($[\mathbf{23}]^{3+}$) and $[Ru_2(btpyxa)(Bu_2Sq)_2(\mu\text{-}O)]^{3+}$ ($[\mathbf{24}]^{3+}$).

In addition, installation of a more flexible bridging ligand instead of the btpyan ligand of $[\mathbf{22}]^{2+}$ gives an oxo-bridged complex without any catalytic activity, which indicate the critical importance of the rigid framework of the btpyan ligand for the efficient catalysis.[100] The utilization of 2,7-di-*tert*-butyl-9,9-dimethyl-4,5-bis(2,2′:6′,2″-terpyrid-4′-yl)xanthene (btpyxa) instead of btpyan does not lead to the formation of dihydroxo or diaquo complexes, but an oxo-bridged one, $[Ru^{III}_2(btpyxa)(Bu_2Sq)_2(\mu\text{-}O)]^{3+}$ ($[\mathbf{24}]^{3+}$) (Figure 7). The CV of $[\mathbf{24}]^{3+}$ in CH_2Cl_2 shows four quasi-reversible redox couples at +0.63 V, –0.01 V, –0.30 V, and –0.80 V (vs. SCE), where the first two waves are corresponding to the $[Ru^{IV}–Ru^{III}]/[Ru^{IV}–Ru^{IV}]$ and $[Ru^{III}–Ru^{III}]/[Ru^{IV}–Ru^{III}]$ couples, respectively. Despite the generation of the higher oxidation states of the Ru centers, $[\mathbf{24}]^{3+}$ exhibits no catalytic activity in the water oxidation, which strongly supports the necessity of the rigid btpyan ligand of $[\mathbf{22}]^{2+}$ to separate the two hydroxo moieties by a suitable distance.

Because of the remarkable catalytic activity of $[\mathbf{22}]^{2+}$, several theoretical studies have been carried out recently to reveal the reaction mechanism of the water oxidation, especially the most crucial step, the O–O bond formation.[101–103] The most plausible mechanism of the O–O bond formation so far is based on the radical coupling between the two oxyl radicals triggered by spin inversion on the Ru(III) centers (Scheme 5).[101] Acid-base equilibrium of the aqua ligands coupled with an electron transfer (ET) to the quinone ligands gives the tetraradical complex $[Ru^{II}_2(btpyan)(Bu_2Sq)_2(O^{\bullet-})_2]$. As described above, the facile O–O bond formation is suppressed in the tetraradical species because of a local triplet diradical (LTD) state of the two oxyl radicals (Hund's rule). The two-electron removal from the two closed-shell Ru(II) centers to open-shell Ru(III), however, generates $[Ru^{III}_2(btpyan)(Bu_2Sq)_2(O^{\bullet-})_2]^{2+}$ bearing six unpaired electrons. The computational study shows that the unpaired electron on the oxyl radical in these species couples ferromagnetically with that on the adjacent Ru(III) center. The spin on the Ru(III) undergoes facile inversion (SI) due to a heavy atom effect, which thus induces concomitant inversion of the magnetically coupled spin on the neighboring $O^{\bullet-}$. As a result, the two oxyl radicals afford a local singlet diradical (LSD) pair that readily couples to form an O–O bond (RC) to give a peroxide species (O_2^{2-}). The mononuclear counterpart $[\mathbf{21a}]^{2+}$ does not exhibit any catalytic activity in water oxidation despite the absence of this quantum constraint for intermolecular radical coupling, which is presumably because of electrostatic repulsion between the anionic oxyl radicals.

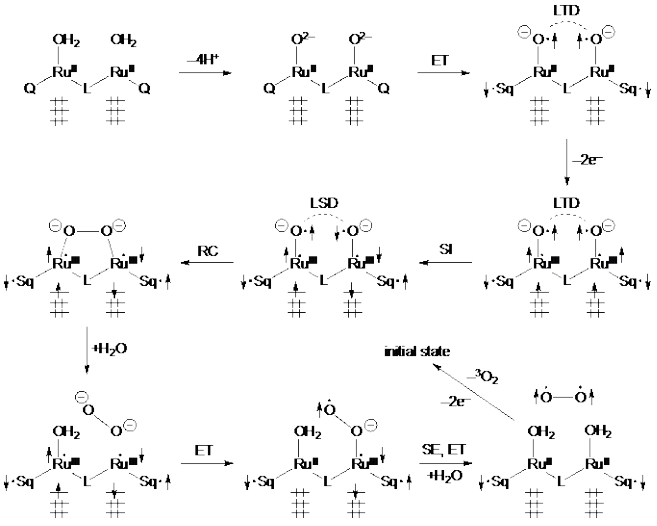

Scheme 5. A radical coupling mechanism for the O–O bond formation in the water splitting by $[\mathbf{22}]^{2+}$ proposed by Tanaka and co-workers[101] (L: btpyan; Q (Sq): 3,6-di-*tert*-butyl-1,2-benzo(semi)quinone).

The following substitution of the peroxide ligand by a water molecule is the rate-limiting step in the catalytic cycle owing to severe steric hindrance of the bulky btpyan and dioxolene ligands. Although the detailed reaction mechanism leading to the O_2 release is still under investigation, one possible pathway is depicted in Scheme 5. After the nucleophilic substitution of one of the oxygen atom of the peroxide by H_2O, one electron transfer from the terminal oxygen to the Ru(III) center will takes place to give a superoxide anion ($O_2^{\bullet-}$). Before another one electron transfer and H_2O attack, a spin exchange (SE) between the Ru(III) center and the semiquinone ligand should occur, and thus a triplet dioxygen will be released accompanied by the recovery of the initial catalyst $[\mathbf{21}]^{2+}$. Taking into account the fact that the O–O bond formation is considered to be the rate-determining step in most of the water oxidation catalyzed by dinuclear or mononuclear metal complexes, the radical coupling mechanism of $[\mathbf{22}]^{2+}$ is a highly efficient pathway of water activation to form an O–O bond.

7. Conclusion

In this microreview, we have focused on the developments and mechanistic studies on the artificial oxygen-evolving catalysts. Many of the homogeneous water oxidation catalysts having been studied so far require an excess (10^5–10^6) of Ce(IV) as a sacrificial oxidant in the highly acidic media, but the harsh conditions often shorten the lifetime of the catalysts. Moreover, it is proposed that the Ce(IV) ion sometimes plays an essential role in the O–O bond formation step in the catalytic cycles (Scheme 1c), and hence the reactions often do not proceed with other oxidants or by electrolytic oxidation. Thus, we suggest that we should refrain from the use of Ce(IV) oxidants in the test systems of the catalysts in view of the application of the catalysts to electrolytic or photocatalytic water splitting.

Here we have focused on the mononuclear and dinuclear ruthenium complexes reported by Tanaka and co-workers, which show remarkable catalytic activities in the water electrolysis. In the mononuclear complex $[\mathbf{20}]^{+}$, the protonation of the pad ligand gives rise to the ruthenium-carbene species, which allows the formation of the Ru(IV) state at the mild potential. It is noteworthy that the use of Ce(IV) as the sacrificial oxidant largely promotes the water oxidation by $[\mathbf{20}]^{+}$ compared to the electrolysis, which suggests the unusual participation of the Ce(IV) ion in the reaction. In the dinuclear complex $[\mathbf{22}]^{2+}$, the dioxolene ligands on the ruthenium centers play essential roles to stabilize Ru–$O^{\bullet-}$ species by the electron delocalization. The resultant Ru–$O^{\bullet-}$ species fixed in spatial proximity smoothly couple to form the O–O bond upon the oxidation of ruthenium ions and the following spin inversion on the metal centers. This is the first example of the water oxidation catalyst in which the O–O bond formation mechanism including the coupling of the metal-oxyl radical species has been elucidated. Recent studies have proposed that the O–O bond formation process in the natural OEC might include a radicaloid intermediate Mn=$O^{\bullet}$.[104–106] In addition, very recently, it has been suggested that some artificial water oxidation catalysts, including "blue dimer", even involve M=$O^{\bullet}$ radical(oid) species in their O–O bond forming transformations.[34,42,107] Piecing together these insights, we can speculate that the metal-oxyl radical complexes will be more common species as we have considered, and might be involved in other oxidation reactions processed by both natural metalloenzymes and artificial metal catalysts.

[1] J. Chow, R. J. Kopp, P. R. Portney, *Science* **2003**, *302*, 1528–1531.

[2] N. S. Lewis, D. G. Nocera, *Proc. Natl. Acad. Sci. USA* **2006**, *103*, 15729–15735.

[3] J. J. Concepcion, R. L. House, J. M. Papanikolas, T. J. Meyer, *Proc. Natl. Acad. Sci. USA* **2012**, *109*, 15560–15564.

[4] M. G. Walter, E. L. Warren, J. R. McKone, S. W. Boettcher, Q. Mi, E. A. Santori, N. S. Lewis, *Chem. Rev.* **2010**, *110*, 6446–6473.

[5] T. R. Cook, D. K. Dogutan, S. Y. Reece, Y. Surendranath, T. S. Teets, D. G. Nocera, *Chem. Rev.* **2010**, *110*, 6474–6502.

[6] W. Rüttinger, G. C. Dismukes, *Chem. Rev.* **1997**, *97*, 1–24.

[7] M. Yagi, M. Kaneko, *Chem. Rev.* **2001**, *101*, 21–35.

[8] H. Lv, Y. V. Geletii, C. Zhao, J. W. Vickers, G. Zhu, Z. Luo, J. Song, T. Lian, D. G. Musaev, C. L. Hill, *Chem. Soc. Rev.* **2012**, *41*, 7572–7589.

[9] B. Kok, B. Forbush, M. McGloin, *Photochem. Photobiol.* **1970**, *11*, 457–475.

[10] J. Barber, *Chem. Soc. Rev.* **2009**, *38*, 185–196.

[11] J. P. McEvoy, G. W. Brudvig, *Chem. Rev.* **2006**, *106*, 4455–4483.

[12] Y. Umena, K. Kawakami, J.-R. Shen, N. Kamiya, *Nature* **2011**, *473*, 55–60.

[13] S. W. Gersten, G. J. Samuels, T. J. Meyer, *J. Am. Chem. Soc.* **1982**, *104*, 4029–4030.

[14] J. A. Gilbert, D. S. Eggleston, W. R. Murphy, Jr., D. A. Geselowitz, S. W. Gersten, D. J. Hodgson, T. J. Meyer, *J. Am. Chem. Soc.* **1985**, *107*, 3855–3864.

[15] D. Geselowitz, T. J. Meyer, *Inorg. Chem.* **1990**, *29*, 3894–3896.

[16] K. Nagoshi, M. Yagi, M. Kaneko, *Bull. Chem. Soc. Jpn.* **2000**, *73*, 2193–2197.

[17] M. Yagi, M. Kasamatsu, M. Kaneko, *J. Mol. Catal. A* **2000**, *151*, 29–35.

[18] C. Sens, I. Romero, M. Rodríguez, A. Llobet, T. Parella, J. Benet-Buchholz, *J. Am. Chem. Soc.* **2004**, *126*, 7798–7799.

[19] F. Bozoglian, S. Romain, M. Z. Ertem, T. K. Todorova, C. Sens, J. Mola, M. Rodríguez, I. Romero, J. Benet-Buchholz, X. Fontrodona, C. J. Cramer, L. Gagliardi, A. Llobet, *J. Am. Chem. Soc.* **2009**, *131*, 15176–15187.

[20] X. Sala, I. Romero, M. Rodríguez, L. Escriche, A. Llobet, *Angew. Chem. Int. Ed.* **2009**, *48*, 2842–2852.

[21] R. Zong, R. P. Thummel, *J. Am. Chem. Soc.* **2005**, *127*, 12802–12803.

[22] Z. Deng, H.-W. Tseng, R. Zong, D. Wang, R. Thummel, *Inorg. Chem.* **2008**, *47*, 1835–1848.

[23] Y. Xu, A. Fischer, L. Duan, L. Tong, E. Gabrielsson, B. Åkermark, L. Sun, *Angew. Chem. Int. Ed.* **2010**, *49*, 8934–8937.

[24] Y. Xu, T. Åkermark, V. Gyollai, D. Zou, L. Eriksson, L. Duan, R. Zhang, B. Åkermark, L. Sun, *Inorg. Chem.* **2009**, *48*, 2717–2719.

[25] Y. V. Geletii, B. Botar, P. Kögerler, D. A. Hillesheim, D. G. Musaev, C. L. Hill, *Angew. Chem. Int. Ed.* **2008**, *47*, 3896–3899.

[26] A. Sartorel, M. Carraro, G. Scorrano, R. D. Zorzi, S. Geremia, N. D. McDaniel, S. Bernhard, M. Bonchio, *J. Am. Chem. Soc.* **2008**, *130*, 5006–5007.

[27] Y. Naruta, M. Sasayama, T. Sasaki, *Angew. Chem. Int. Ed. Engl.* **1994**, *33*, 1839–1841.

[28] Y. Shimazaki, T. Nagano, H. Takesue, B.-H. Ye, F. Tani, Y. Naruta, *Angew. Chem. Int. Ed.* **2003**, *43*, 98–100.

[29] J. Limburg, J. S. Vrettos, L. M. Liable-Sands, A. L. Rheingold, R. H. Crabtree, G. W. Brudvig, *Science* **1999**, *283*, 1524–1527.

[30] J. Limburg, J. S. Vrettos, H. Chen, J. C. de Paula, R. H. Crabtree, G. W. Brudvig, *J. Am. Chem. Soc.* **2001**, *123*, 423–430.

[31] R. Tagore, R. H. Crabtree, G. W. Brudvig, *Inorg. Chem.* **2008**, *47*, 1815–1823.

[32] M. Yagi, K. Narita, *J. Am. Chem. Soc.* **2004**, *126*, 8084–8085.

[33] A. K. Poulsen, A. Rompel, C. J. McKenzie, *Angew. Chem. Int. Ed.* **2005**, *44*, 6916–6920.

[34] Y. Gao, R. H. Crabtree, G. W. Brudvig, *Inorg. Chem.* **2012**, *51*, 4043–4050.

[35] M. Wiechen, H.-M. Berends, P. Kurz, *Dalton Trans.* **2012**, *41*, 21–31.

[36] J. P. Collins, J. P. Sauvage, *Inorg. Chem.* **1986**, *25*, 135–141.

[37] N. D. McDaniel, F. J. Coughlin, L. L. Tinker, S. Bernhard, *J. Am. Chem. Soc.* **2008**, *130*, 210–217.

[38] H.-W. Tseng, R. Zong, J. T. Muckerman, R. Thummel, *Inorg. Chem.* **2008**, *47*, 11763–11773.

[39] J. J. Concepcion, J. W. Jurss, J. L. Templeton, T. J. Meyer, *J. Am. Chem. Soc.* **2008**, *130*, 16462–16463.

[40] J. J. Concepcion, J. W. Jurss, M. R. Norris, Z. Chen, J. L. Templeton, T. J. Meyer, *Inorg. Chem.* **2010**, *49*, 1277–1279.

[41] S. Masaoka, K. Sakai, *Chem. Lett.* **2009**, *38*, 182–183.

[42] M. Yoshida, S. Masaoka, J. Abe, K. Sakai, *Chem. Asian J.* **2010**, *5*, 2369–2378.

[43] J. F. Hull, D. Balcells, J. D. Blakemore, C. D. Incarvito, O. Eisenstein, G. W. Brudvig, R. H. Crabtree, *J. Am. Chem. Soc.* **2009**, *131*, 8730–8731.

[44] R. Lalrempuia, N. D. McDaniel, H. Müller-Bunz, S. Bernhard, M. Albrecht, *Angew. Chem. Int. Ed.* **2010**, *49*, 9765–9768.

[45] L. Duan, C. M. Araujo, M. S. G. Ahlquist, L. Sun, *Proc. Natl. Acad. Sci. USA*, **2012**, *109*, 15584–15588.

[46] L. Duan, F. Bozoglian, S. Mandal, B. Stewart, T. Privalov, A. Llobet, L. Sun, *Nat. Chem.* **2012**, *4*, 418–423.

[47] L. Duan, A. Fischer, Y. Xu, L. Sun, *J. Am. Chem. Soc.* **2009**, *131*, 10397–10399.

[48] Y. Gao, X. Ding, J. Liu, L. Wang, Z. Lu, L. Li, L. Sun, *J. Am. Chem. Soc.* **2013**, *135*, 4219–4222.

[49] Q. Yin, J. M. Tan, C. Besson, Y. V. Geletii, D. G. Musaev, A. E. Kuznetsov, Z. Luo, K. I. Hardcastle, C. L. Hill, *Science* **2010**, *328*, 342–345.

[50] D. K. Dogutan, R. McGuire, D. G. Nocera, *J. Am. Chem. Soc.* **2011**, *133*, 9178–9180.

[51] D. J. Wasylenko, C. Ganesamoorthy, J. Borau-Garcia, C. P. Berlinguette, *Chem. Commun.* **2011**, *47*, 4249–4251.

[52] T. Nakazono, A. R. Parent, K. Sakai, *Chem. Commun.* **2013**, DOI: 10.1039/C3CC43031F.

[53] S. M. Barnett, K. I. Goldberg, J. M. Mayer, *Nat. Chem.* **2012**, *4*, 498–502.

[54] J. Lloret-Fillol, Z. Codolà, I. Garcia-Bosch, L. Gómez, J. J. Pla, M. Costas, *Nat. Chem.* **2011**, *3*, 807–813.

[55] W. C. Ellis, N. D. McDaniel, S. Bernhard, T. J. Collins, *J. Am. Chem. Soc.* **2010**, *132*, 10990–10991.

[56] G. Chen, L. Chen, S.-M. Ng, W.-L. Man, T.-C. Lau, *Angew. Chem. Int. Ed.* **2013**, *52*, 1789–1791.

[57] Z. Codolà, I. Garcia-Bosch, F. Acuña-Parés, I. Prat, J. M. Luis, M. Costas, J. Lloret-Fillol, *Chem. Eur. J.* **2013**, DOI: 10.1002/chem.201301112.

[58] J. K. Hurst, *Coord. Chem. Rev.* **2005**, *249*, 313–328.

[59] F. Liu, J. J. Concepcion, J. W. Jurss, T. Cardolaccia, J. L. Templeton, T. J. Meyer, *Inorg. Chem.* **2008**, *47*, 1727–1752.

[60] J. K. Hurst, J. L. Cape, A. E. Clark, S. Das, C. Qin, *Inorg. Chem.* **2008**, *47*, 1753–1764.

[61] J. K. Hurst, J. Zhou, Y. Lei, *Inorg. Chem.* **1992**, *31*, 1010–1017.

[62] Y. Lei, J. K. Hurst, *Inorg. Chem.* **1994**, *33*, 4460–4467.

[63] H. Yamada, J. K. Hurst, *J. Am. Chem. Soc.* **2000**, *122*, 5303–5311.

[64] H. Yamada, W. F. Siems, T. Koike, J. K. Hurst, *J. Am. Chem. Soc.* **2004**, *126*, 9786–9795.

[65] X. Yang, M.-H. Baik, *J. Am. Chem. Soc.* **2006**, *128*, 7476–7485.

[66] J. L. Cape, S. V. Lymar, T. Lightbody, J. K. Hurst, *Inorg. Chem.* **2009**, *48*, 4400–4410.

[67] J. L. Cape, J. K. Hurst, *J. Am. Chem. Soc.* **2008**, *130*, 827–829.

[68] L. Tong, A. K. Inge, L. Duan, L. Wang, X. Zou, L. Sun, *Inorg. Chem.* **2013**, *52*, 2505–2518.

[69] M. Murakami, D. Hong, T. Suenobu, S. Yamaguchi, T. Ogura, S. Fukuzumi, *J. Am. Chem. Soc.* **2011**, *133*, 11605–11613.

[70] A. Sartorel, P. Miró, E. Salvadori, S. Romain, M. Carraro, G. Scorrano, M. D. Valentin, A. Llobet, C. Bo, M. Bonchio, *J. Am. Chem. Soc.* **2009**, *131*, 16051–16053.

[71] A. E. Kuznetsov, Y. V. Geletii, C. L. Hill, K. Morokuma, D. G. Musaev, *J. Am. Chem. Soc.* **2009**, *131*, 6844–6854.

[72] J. J. Concepcion, M.-K. Tsai, J. T. Muckerman, T. J. Meyer, *J. Am. Chem. Soc.* **2010**, *132*, 1545–1557.

[73] A. Kimoto, K. Yamauchi, M. Yoshida, S. Masaoka, K. Sakai, *Chem. Commun.* **2012**, *48*, 239–241.

[74] J. A. Stull, R. D. Britt, J. L. McHale, F. J. Knorr, S. V. Lymar, J. K. Hurst, *J. Am. Chem. Soc.* **2012**, *134*, 19973–19976.

[75] D. E. Polyansky, J. T. Muckerman, J. Rochford, R. Zong, R. P. Thummel, E. Fujita, *J. Am. Chem. Soc.* **2011**, *133*, 14649–14665.

[76] X. Li, G. Chen, S. Schinzel, P. E. M. Siegbahn, *Dalton Trans.* **2011**, *40*, 11296–11307.

[77] S. Romain, F. Bozoglian, X. Sala, A. Llobet, *J. Am. Chem. Soc.* **2009**, *131*, 2768–2769.

[78] S. Maji, L. Vigara, F. Cottone, F. Bozoglian, J. Benet-Buchholz, A. Llobet, *Angew. Chem. Int. Ed.* **2012**, *51*, 5967–5970.

[79] D. J. Wasylenko, C. Ganesamoorthy, M. A. Henderson, B. D. Koivisto, H. D. Osthoff, C. P. Berlinguette, *J. Am. Chem. Soc.* **2010**, *132*, 16094–16106.

[80] D. J. Wasylenko, C. Ganesamoorthy, M. A. Henderson, C. P. Berlinguette, *Inorg. Chem.* **2011**, *50*, 3662–3672.

[81] S. K. Padhi, K. Kobayashi, S. Masuno, K. Tanaka, *Inorg. Chem.* **2011**, *50*, 5321–5323.

[82] S. K. Padhi, K. Tanaka, *Inorg. Chem.* **2011**, *50*, 10718–10723.

[83] S. K. Padhi, R. Fukuda, M. Ehara, K. Tanaka, *Inorg. Chem.* **2012**, *51*, 5386–5392.

[84] S. K. Padhi, R. Fukuda, M. Ehara, K. Tanaka, *Inorg. Chem.* **2012**, *51*, 8091–8102.

[85] J. Mola, E. Mas-Marza, X. Sala, I. Romero, M. Rodríguez, C. Viñas, T. Parella, A. Llobet, *Angew. Chem. Int. Ed.* **2008**, *47*, 5830–5832.

[86] C. G. Pierpont, R. M. Buchanan, *Coord. Chem. Rev.* **1981**, *38*, 45–87.

[87] A. Dei, D. Gatteschi, C. Sangregorio, L. Sorace, *Acc. Chem. Res.* **2004**, *37*, 827–835.

[88] E. Evangelio, D. Ruiz-Molina, *Eur. J. Inorg. Chem.* **2005**, 2957–2971.

[89] J. L. Boyer, J. Rochford, M.-K. Tsai, J. T. Muckerman, E. Fujita, *Coord. Chem. Rev.* **2010**, *254*, 309–330.

[90] S. Bhattacharya, S. R. Boone, G. A. Fox, C. G. Pierpont, *J. Am. Chem. Soc.* **1990**, *112*, 1088–1096.

[91] T. Wada, M. Yamanaka, T. Fujihara, Y. Miyazato, K. Tanaka, *Inorg. Chem.* **2006**, *45*, 8887–8894.

[92] M. Haga, E. S. Dodsworth, A. B. P. Lever, *Inorg. Chem.* **1986**, *25*, 447–453.

[93] K. Kobayashi, H. Ohtsu, T. Wada, T. Kato, K. Tanaka, *J. Am. Chem. Soc.* **2003**, *125*, 6729–6739.

[94] K. Kobayashi, H. Ohtsu, T. Wada, K. Tanaka, *Chem. Lett.* **2002**, *31*, 868–869.

[95] T. Wada, K. Tsuge, K. Tanaka, *Chem. Lett.* **2000**, *29*, 910–911.

[96] T. Wada, K. Tsuge, K. Tanaka, *Inorg. Chem.* **2001**, *40*, 329–337.

[97] T. Wada, K. Tsuge, K. Tanaka, *Angew. Chem. Int. Ed.* **2000**, *39*, 1479–1482.

[98] T. Wada, J. T. Muckerman, E. Fujita, K. Tanaka, *Dalton Trans.* **2011**, *40*, 2225–2233.

[99] T. Wada, H. Ohtsu, K. Tanaka, *Chem. Eur. J.* **2012**, *18*, 2374–2381.

[100] T. Wada, K. Tanaka, *Eur. J. Inorg. Chem.* **2005**, 3832–3839.

[101] K. Tanaka, H. Isobe, S. Yamanaka, K. Yamaguchi, *Proc. Natl. Acad. Sci. USA* **2012**, *109*, 15600–15605.

[102] J. T. Muckerman, D. E. Polyansky, T. Wada, K. Tanaka, E. Fujita, *Inorg. Chem.* **2008**, *47*, 1787–1802.

[103] S. Ghosh, M.-H. Baik, *Inorg. Chem.* **2011**, *50*, 5946–5957.

[104] K. Yamaguchi, Y. Takahara, T. Fueno in *Applied Quantum Chemistry* (Eds.: V. H. Smith, Jr., H. F. Schaefer, III, K. Morokuma), D. Reidel Pub. Co., Dordrecht, **1986**, pp. 155–184.

[105] P. E. M. Siegbahn, *Inorg. Chem.* **2008**, *47*, 1779–1786.

[106] P. E. M. Siegbahn, *Acc. Chem. Res.* **2009**, *42*, 1871–1880.

[107] D. Moonshiram, I. Alperovich, J. J. Concepcion, T. J. Meyer, Y Pushkar, *Proc. Natl. Acad. Sci. USA*, **2013**, *110*, 3765–3770.

Received: ((will be filled in by the editorial staff))
Published online: ((will be filled in by the editorial staff))

The selected current literature in homogeneous molecular catalysts for water oxidation based on transition metal complexes is reviewed. Special attention is paid to the mechanism of the O–O bond formation in ruthenium-based catalysts. This review surveys rational approaches to conducting oxygen evolution near the thermodynamic limit.

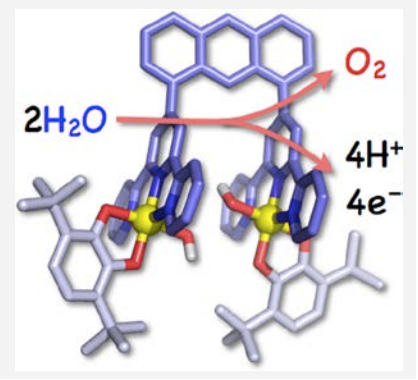

Takashi Kikuchi and Koji Tanaka*

…….. Page No. – Page No.

Recent Advance in Molecular Catalysts for Water Oxidation

Keywords: Water splitting / Oxidation / Homogeneous catalysis / Electrochemistry / Reaction mechanisms / Radicals / Ruthenium